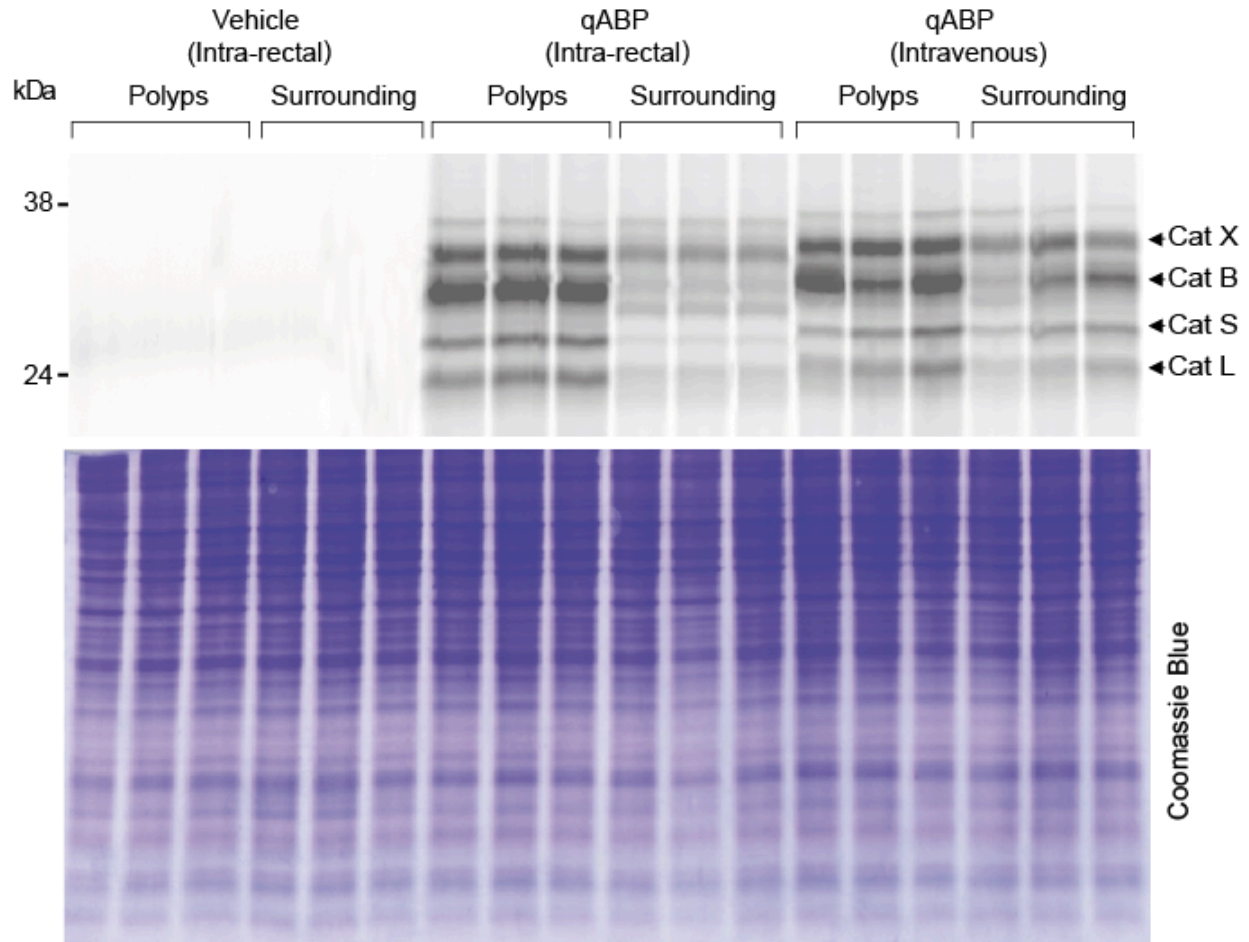


| Parameter                 | Intravenous |                    |
|---------------------------|-------------|--------------------|
|                           |             | 95% CI             |
| Sensitivity               | 87.50%      | 70.99 % to 96.41 % |
| Specificity               | 76.92%      | 46.20 % to 94.69 % |
| Positive likelihood Ratio | 3.79        | 1.39 to 10.32      |
| Negative likelihood Ratio | 0.16        | 0.06 to 0.43       |
| Positive predictive Value | 90.32%      | 74.22 % to 97.85 % |
| Negative predictive Value | 71.43%      | 41.92 % to 91.43 % |

**Table S1 related to Figure 2 and S3.** Values of false positive and false negative rates, sensitivity and specificity of neoplastic adenomas determined by probe labeling. Statistical calculations were performed using 95% confidence intervals.

| Parameter                 | Local (intra-rectal) |                    | Intravenous |                    |
|---------------------------|----------------------|--------------------|-------------|--------------------|
|                           |                      | 95% CI             |             | 95% CI             |
| Sensitivity               | 93.55%               | 78.54 % to 99.02 % | 88.89%      | 73.92 % to 96.82 % |
| Specificity               | 80.00%               | 44.43 % to 96.89 % | 61.54%      | 31.64 % to 86.00 % |
| Positive likelihood Ratio | 4.68                 | 1.35 to 16.21      | 2.31        | 1.15 to 4.64       |
| Negative likelihood Ratio | 0.08                 | 0.02 to 0.32       | 0.18        | 0.07 to 0.50       |
| Positive predictive Value | 93.55%               | 78.54 % to 99.02 % | 86.49%      | 71.21 % to 95.41 % |
| Negative predictive Value | 80.00%               | 44.43 % to 96.89 % | 76.67%      | 34.95 % to 89.87 % |

**Table S2 related to Figure 4 and S4.** Values of false positive and false negative, sensitivity and specificity of neoplastic adenomas labeling by the probe. Statistical calculations were performed using 95% confidence intervals.



**Figure S1, related to figure 4. Analysis of cathepsin labeling in surrounding normal tissue and polyps after intra-rectal or intravenous injection of the qABP.** Samples were analyzed by SDS-PAGE followed flatbed laser scanning of the gel to visualize probe labeled proteins. The intensity of fluorescent signals were quantified as outlined in the methods section and used to generate the graphs shown in Fig. 4D. The lower gel shows scanned image after Coomassie<sup>®</sup> Blue staining as a control for sample loading.

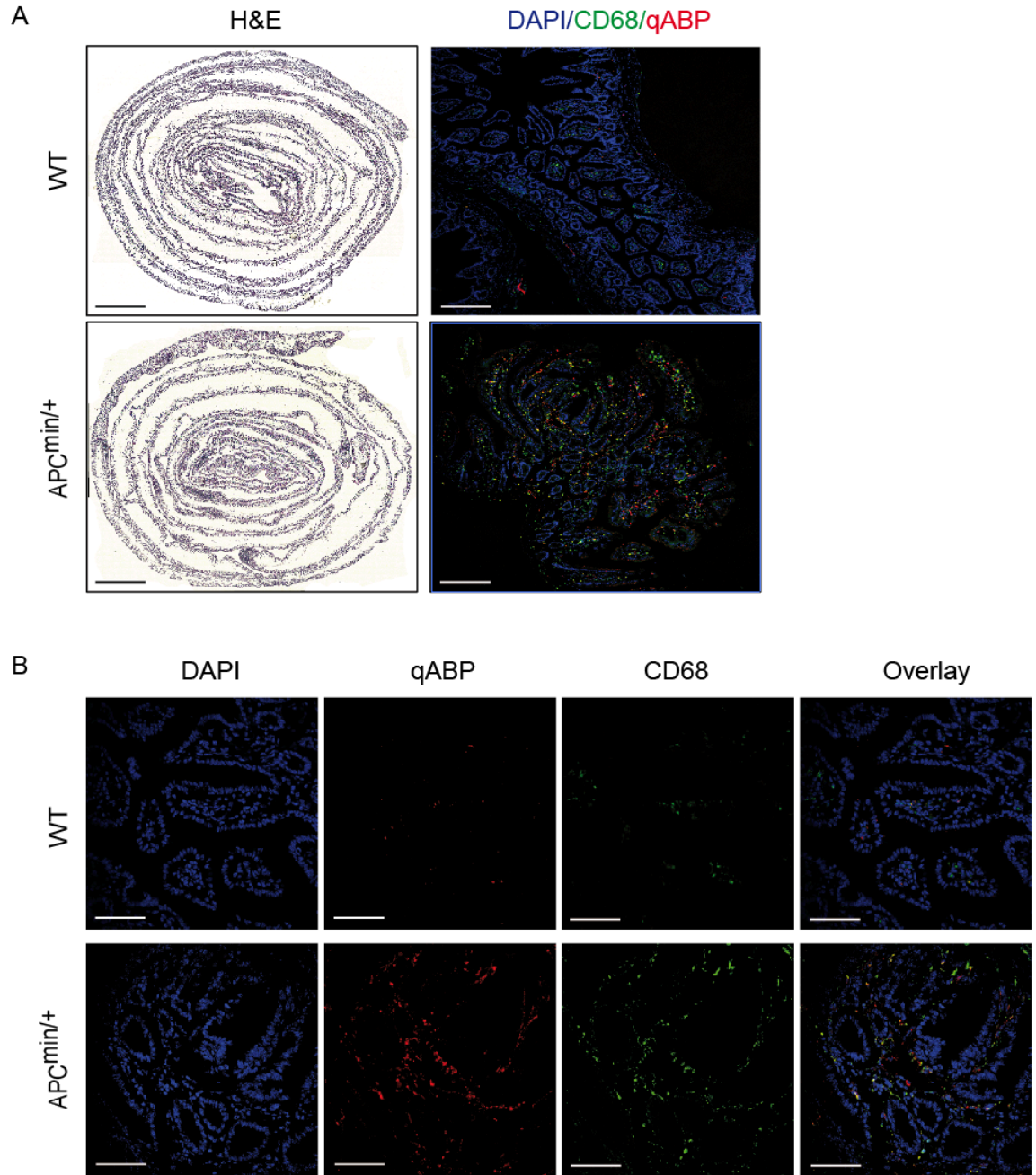


**Figure S2, related to figure 5. Probe labeling is correlated with abnormalities of the intestinal epithelium.** (A) Mosaic images of H&E (left) and immunofluorescence (right) staining of wild type (top) and APC<sup>min/+</sup> (bottom) intestines 1 hour following administration of qABP (red). Samples were co stained with DAPI (blue) and CD68 (green). (Scale bars of H&E and fluorescence images represent 5mm and 200 $\mu$ m respectively). (B) High magnification confocal images of matched samples, wild type (top) and APC<sup>min/+</sup> (bottom) intestines co stained with DAPI (blue) and CD68 (green). (Scale bar represents 20 $\mu$ m).

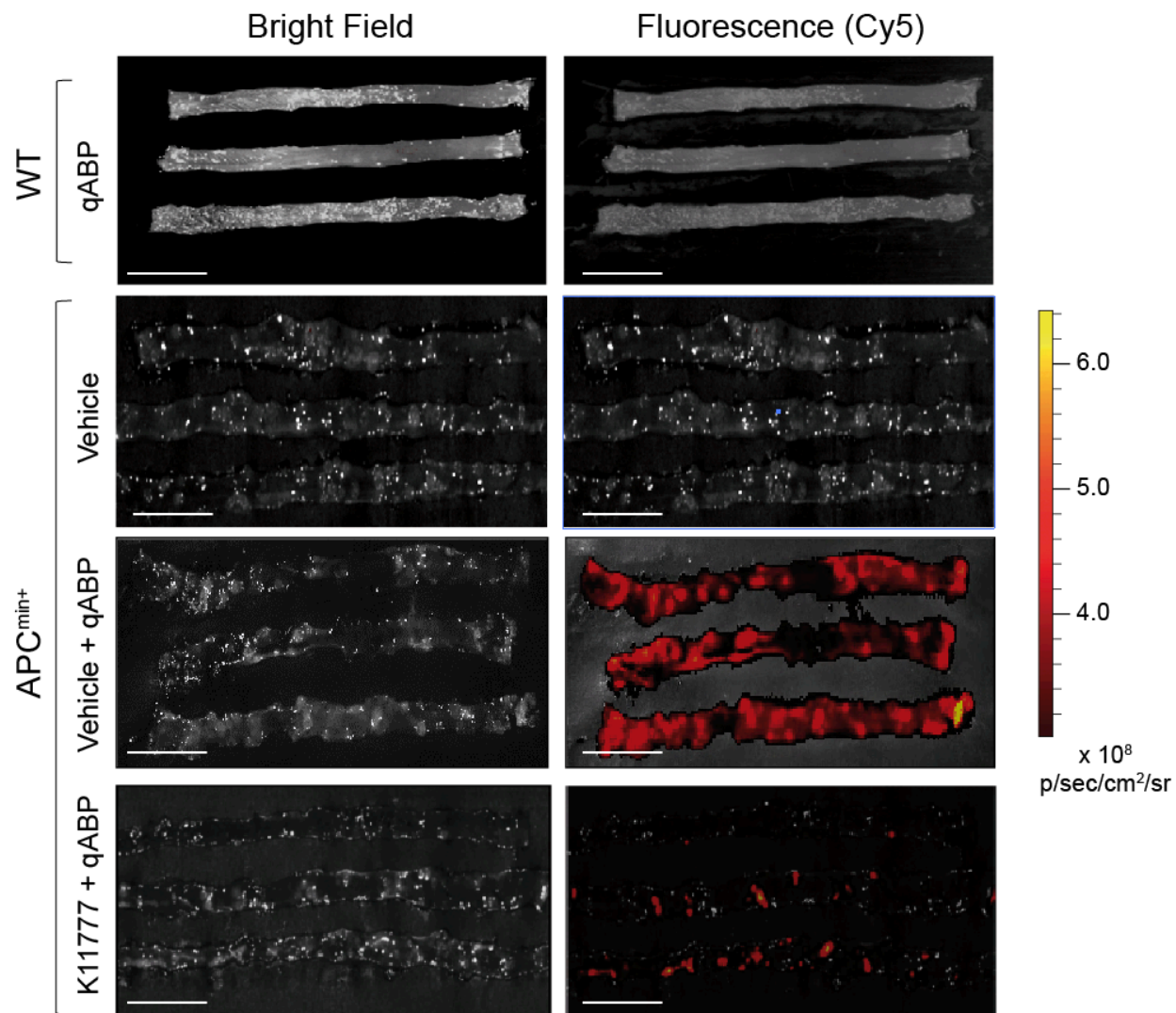


**Figure S3, related to Figure 2 and table S1. The probe accumulates at intestinal neoplasms following intravenous administration.** *Ex vivo* bright field (left) and fluorescence optical images (right) of the intestine tissues of wild-type (WT; top) and APC<sup>min/+</sup> (center to bottom) mice 1 hour post i.v. administration of the probe (scale bar represents 5mm).

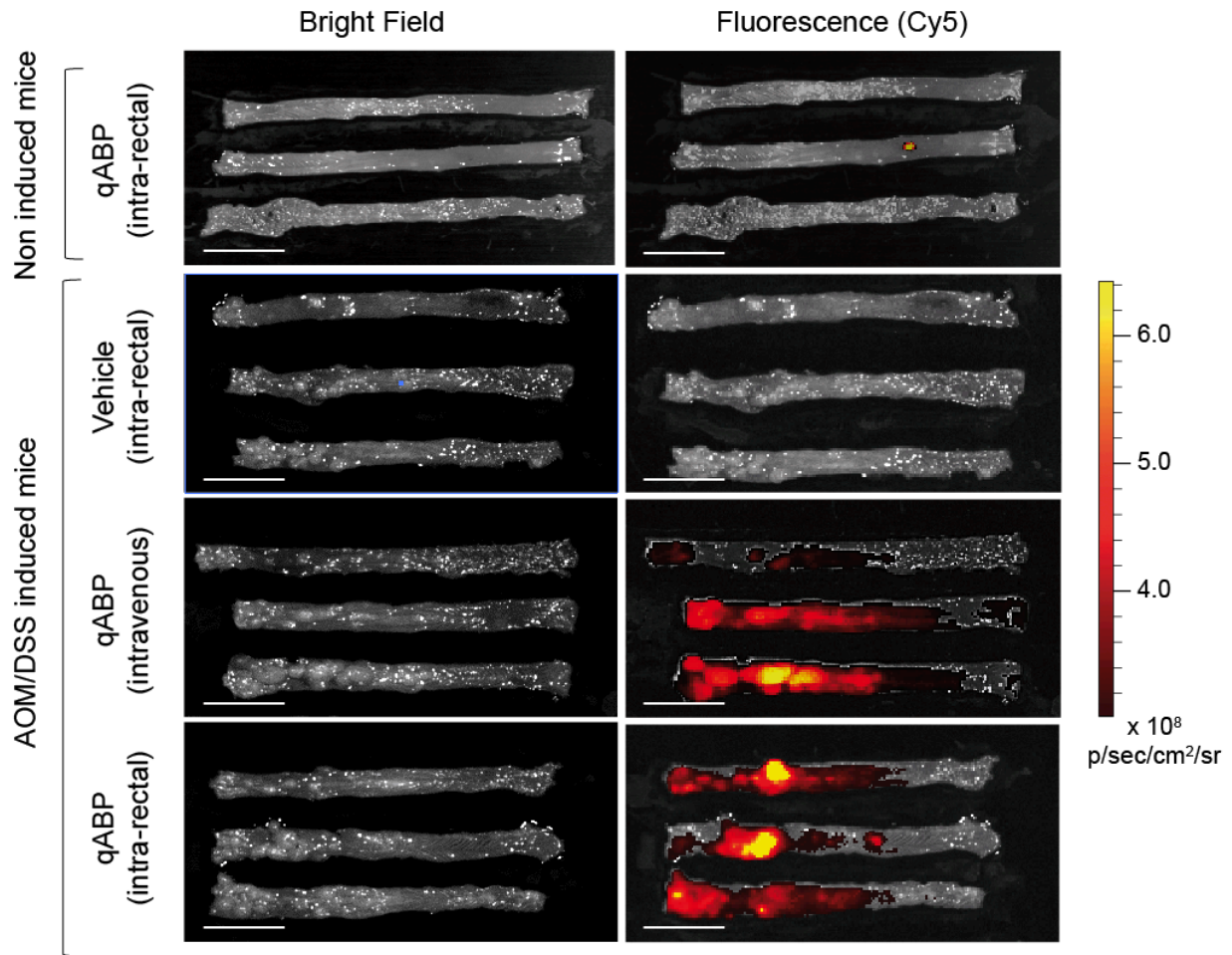


**Figure S4, related to figure 4 and table S2. The probe accumulates at colitis-related colonic neoplasms following intravenous and local (intra-rectal) administration . *Ex vivo* bright field (left) and fluorescence optical images (right) of the colon tissues of wild-type (WT; top) and APC<sup>min/+</sup> (center to bottom) mice 1 hour post i.v. administration of the probe (scale bar represents 5mm).**